An Alternative Approach to the Modification of Talc for the Fabrication of Polypropylene/Talc Composites

Tao Wang, Dan Liu, Joseph L. Keddie

Department of Physics, University of Surrey, Guildford, Surrey GU2 7XH, United Kingdom

Received 21 July 2006; accepted 21 February 2007
DOI 10.1002/app.26462
Published online 20 June 2007 in Wiley InterScience (www.interscience.wiley.com).

ABSTRACT: We report an alternative method to modify talc for use in the fabrication of composites of polypropylene (PP) and talc. Grinding pulverization is employed to prepare talc fillers (referred to hereafter as *p*-talc). The properties of composites made with *p*-talc compare favorably with composites made with pulverized talc that has been further treated with a silane coupling agent (referred to as *s*-talc). The morphology of PP/*p*-talc composites illustrates particle orientation and a uniform dispersion of pulverized talc in the PP matrix. Modulated DSC analysis shows the ability of *p*-talc and *s*-talc to nucleate PP crystallization. The mechanical properties (i.e., the dynamic modulus, tensile strength, and impact resistance) of the PP/*p*-talc composites are very similar to PP/*s*-talc composites. The modification of talc by grinding is thus a highly effective alternative method to prepare PP/talc composites that does not require chemical treatment of the talc. The pulverization method is simpler and less expensive in comparison to silane treatment. © 2007 Wiley Periodicals, Inc. J Appl Polym Sci 106: 386–393, 2007

Key words: PP/talc composites; grinding pulverization; microstructure; crystallization; mechanical properties

INTRODUCTION

Polypropylene (PP) possesses some exceptional properties. It has the highest stiffness, the highest melting point and the best thermal resistance of all the polyolefins.[1] Its applications are greatly extended by adding inorganic filler such as talc, calcium carbonate, mica, and glass to improve mechanical properties, thermal resistance, and dimensional stability, all at a low cost.[2–14]

The performance of polymer/inorganic composites is strongly related to the interfacial adhesion between the polymer and the filler. As PP is a nonpolar, chemically inert polymer, it does not interact with most inorganic fillers and results in poor filler dispersion and weak interfacial adhesion. Consequently, in composites with untreated talc, depressed physical properties are observed.[15]

To overcome the limitations of fabricating composites of talc and polymers, a variety of coupling agents, including silanes,[16] titanium esters,[17] phosphate, aluminate, and zirconate, have been adopted to modify the interfacial structure. Although these coupling agents strongly interact with the filler, their chemical interaction with the nonpolar PP matrix is weak.[18] Qiu et al.[19] employed vinyltrimethoxy silane-grafted PP as a coupling agent to improve the interfacial adhesion of the PP/talc system. It is thought that the polar silane functionality interacts with talc, and the polymeric PP chain is compatible with the bulk PP, thereby inducing a significant increase in the mechanical properties.

Functionalization of the bulk polymer can also enhance the compatibility with inorganic fillers and thus is another way to prepare high performance polymer composites. The usual way to functionalize PP is to graft polar monomers, e.g., maleic anhydride (MA), acrylic acid, glycidyl methcrylate, and styrene,[20,21] onto the PP backbone. Functional polymeric agents can strongly interact with both the filler and PP. However, in the grafting techniques, monomers, and additives must be added. This step can cause chemical pollution during production because of the volatilization of monomers and additives at high temperature as well as during long-term use. For example, the MA grafting process is accompanied by a high degree of volatilization and can potentially harm production workers through exposure. The residual monomers also have negative effects on the thermal, electrical, and toxicity properties of the composite.[22] Moreover, crosslinking and degradation of PP, which is undesirable, may also occur during the grafting process.[23]

Properties of a filled system rely also on the filler dispersion and matrix structure and morphology, in addition to the interfacial structure. Importantly, talc can act as nucleating agent to facilitate polymer crystallization.[16,24,25] Li et al.[26] studied the structure and morphology of talcum-filled HDPE and suggested that silane altered the mechanical properties of the

Correspondence to: T. Wang (t.wang@surrey.ac.uk).
Contract grant sponsors: Universities UK, University of Surrey, Kwan Trust.

filled plastic both through an enhancement of the filler dispersion and through a modification of the matrix morphology. There is a loss of polymer chain mobility resulting from the presence of talc, but at high talc contents, the silane coupling agent counters this mobility reduction. Li questioned the choice of silane as a coupling agent for filled polyolefins in which a relatively low cost-to-performance ratio was desired.[26]

As an alternative to the chemical functionalization of talc, activation may be achieved through the mechanical process of pulverization via grinding. This article reports the effects of pulverized talc (referred to hereafter as *p*-talc) on the morphology and properties of PP. Its effects will be shown in comparison to talc treated with a silane coupling agent (referred to hereafter as *s*-talc).

EXPERIMENTAL

Materials

Isotacic polypropylene (T30S, granular) was provided by Daqing Petrochemistry (China) with a melt index ranging from 2.0 to 4.0 g/min and a density of about 910 kg/m^3. The talc (500 mesh) is a commercially manufactured product provided by Guangxi Longguang Talc Development (China). Silane(γ-(methyl acryloyloxyl)propyl trimethoxyl silane) (KH570, Wuhan University Chem. China), likewise a commercial product, was used as a coupling agent.

Preparation of talc

Original 500 mesh quality talc was pulverized by solid state shearing in grinding equipment (DESI M3S, Estonia) to an average particle size of 1500 mesh to create *p*-talc. For comparison, *s*-talc was made by a surface treatment to *p*-talc with the silane coupling agent. In the treatment, *p*-talc was immersed in a 1 wt % solution of the silane in acetone with vigorous stirring at a constant temperature of 20°C. Reflux was used to avoid acetone loss through vaporization. After refluxing for 2 h, the acetone was vaporized to produce *s*-talc.

Composites preparation and testing

PP and talc were premixed with PP:talc ratios of 100 : 10, 100 : 20, 100 : 30, 100 : 40, and 100 : 50 in a mixing machine) (Zhangjiagang City XinFeng In General Use Machine Manufactory, SRL-Z) to achieve talc concentrations of 9, 16.7, 23.1, 28.6, and 33.3 wt % in the composites, respectively. The mixtures were then processed in a twin-screw extruder (Nanjing Rubber Mach., SJSH-30) at a temperature between 200 and 210°C. The final extruded composites were cooled in a water-bath, dried and granulated to sizes less than 3 mm. After drying, the granules were injection-molded in a screw injection molding machine (Nanjing Rubber Mach., SZ-63/400B) at ~ 210°C to obtain ISO multipurpose test specimens (Type 1A, ISO 3168), and then to prepare three types of test specimens: tensile (150 mm long dog bone, with a center section of 80 mm × 10 mm × 4 mm), flexural (80 mm × 10 mm × 4 mm) and impact test (80 mm × 10 mm × 4 mm).

Tensile properties were measured using a tensile tester (RDT-30A, Shenzhen Reger) with computerized data acquisition, at a cross-head speed of 20 mm/min at room temperature. Flexural strengths were measured using the same equipment, with a span of 50 mm and a cross-head speed of 4 mm/min under the same atmosphere conditions. Izod impact strength was obtained from notched specimens using an impact tester (Shanghai Wuzhong Instrument, JB6). Results were all calculated from the data obtained from six replicate measurements.

Morphology

The structure and morphology of the composites were studied using a scanning electron microscope (JSM-5610LV, JEOL, Datum Ltd, Tokyo, Japan). For SEM analysis, samples were frozen in liquid nitrogen, and fracture surfaces were coated with a layer of palladium alloy prior to examination. Impact fracture surfaces were also examined under SEM. The microscope was operated with an accelerating voltage of 10 kV.

Modulated differential scanning calorimetry

The crystallization temperatures of PP were determined by customized DSC (Q1000, TA Instruments) at a cooling rate of 10°C/min following an isothermal hold at 200°C for 10 min. The melting temperature, T_m, and the degrees of crystallinity, X_c, of PP/talc composites were determined by modulated DSC operating at a heating rate of 3°C/min from −50 to 200°C, with a modulation period of 60 s and an amplitude of ±0.7°C. In the MDSC experiments, the endothermic heat flow ΔH_{diff} of the initially existing crystallites can be easily calculated as $\Delta H_{\text{diff}} = \Delta H_{\text{rev}} - \Delta H_{\text{nonrev}}$, where ΔH_{rev} is the endothermic melting (reversing) enthalpy from the reversing heat flow profile, and ΔH_{nonrev} is the exothermic ordering/crystallization (nonreversing) enthalpy from the nonreversing heat flow profile. X_c was thus calculated as $\Delta H_{\text{diff}}/\Delta H_0$, where ΔH_0 is the heat flow of 100% crystalline PP and was taken to be 209 J/g.[27] In the case of talc-filled PP composites, the reversing and nonreversing enthalpies were calculated for the crystallization originating from only the matrix PP. Thus the crystallinity was calculated as

$$X_c = \frac{\Delta H_{\text{diff}}}{\Delta H_0 \times \omega} \quad (1)$$

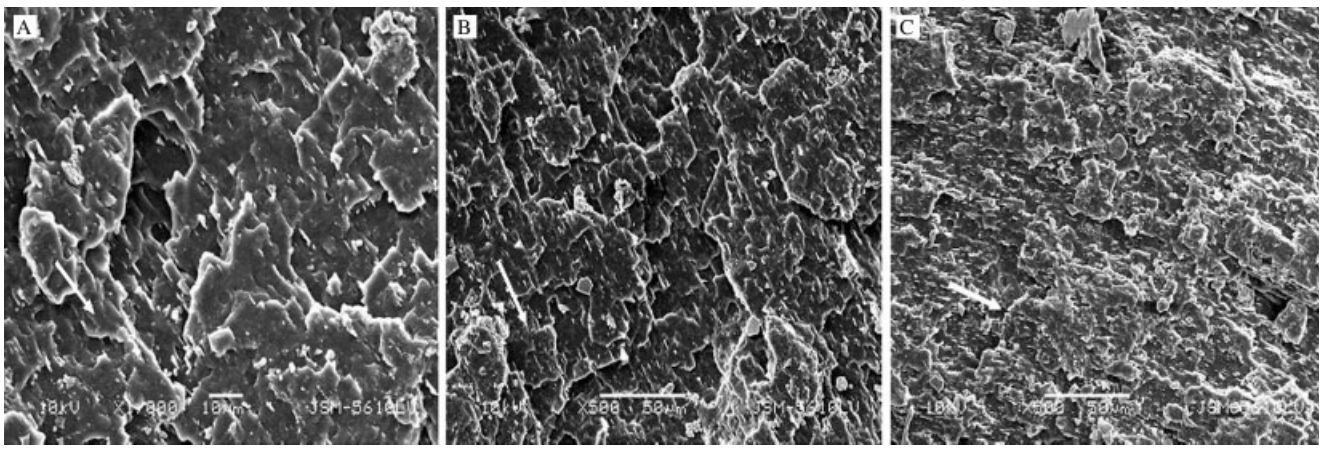

Figure 1 SEM images of freeze-fracture surfaces of the PP/*p*-talc composites with various talc content: (A) 9 wt %; (B) 23.1 wt %; (B) 33.3 wt % (The arrows in the micrograph illustrate talc orientation).

where ω is the weight fraction of PP in the composite.

Dynamic mechanical analysis

Dynamic mechanical analysis (DMA) was conducted at 1 Hz on a DMA Q800 (TA Instruments) instrument using a single cantilever bending method. The heating rate was 3°C min, ramping from −50 to 100°C. The storage modulus (E'), loss modulus (E''), and tan δ (E''/E') were recorded for the two kinds of PP/talc composites.

RESULTS AND DISCUSSION

Dispersion and orientation of pulverized talc in PP matrix

The SEM micrographs in Figure 1(a) reveal the distribution and orientation of *p*-talc in PP at various talc contents. It can be seen from the micrographs that the flake-like talc is dispersed uniformly in the matrix and preferentially along one direction. This uniform dispersion is not decreased even with talc contents as high as 33.3 wt %. Generally, the flow profile in injection-molding will affect the orientation of anisotropic fillers, such as fiber, mica or talc, in a polymer matrix.[28] It is clear in Figure 1 that the talc is distributed in PP along one direction rather than randomly. The arrows point in various directions, because each sample is oriented in a different direction within the SEM chamber. Figure 2 illustrates the dispersion of *s*-talc in PP composites. *S*-talc also disperses in PP in a certain direction. A higher magnification SEM morphology of *s*-talc at 33.3 wt % content [Fig. 2(c)] in PP composite shows aggregation of *s*-talc in some area. At high *p*-talc content, this talc aggregation also exits. This weak talc/talc contact might decrease the performance. Judging from the observed morphology, the grinding pulverization process leads to a good disper-

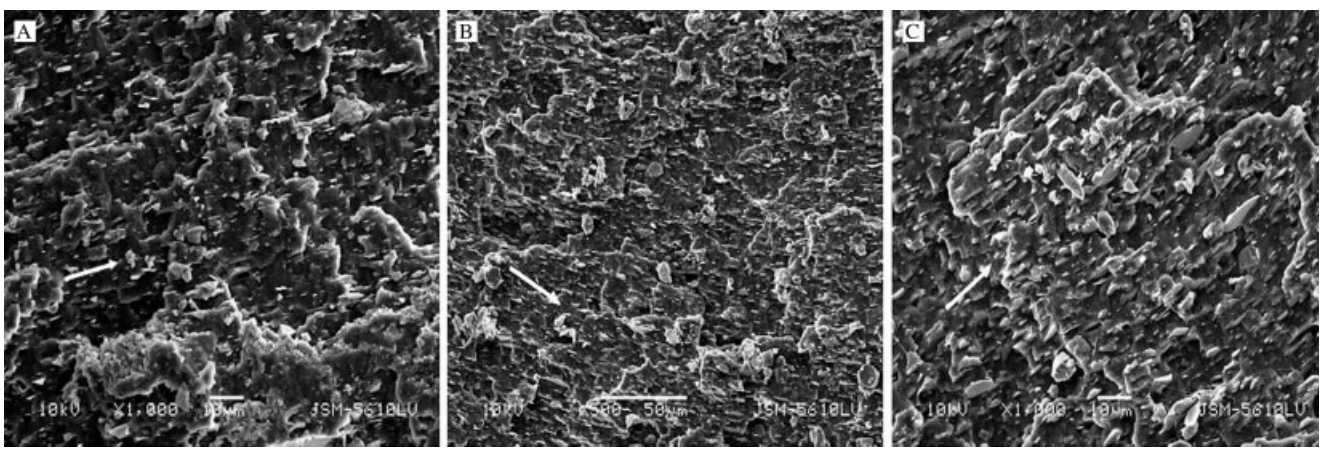

Figure 2 SEM images of freeze-fracture surfaces of the PP/*s*-talc composites with various talc content: (A) 9 wt %; (B) 23.1 wt %; (C) 33.3 wt % (The arrows in the micrograph illustrate talc orientation).

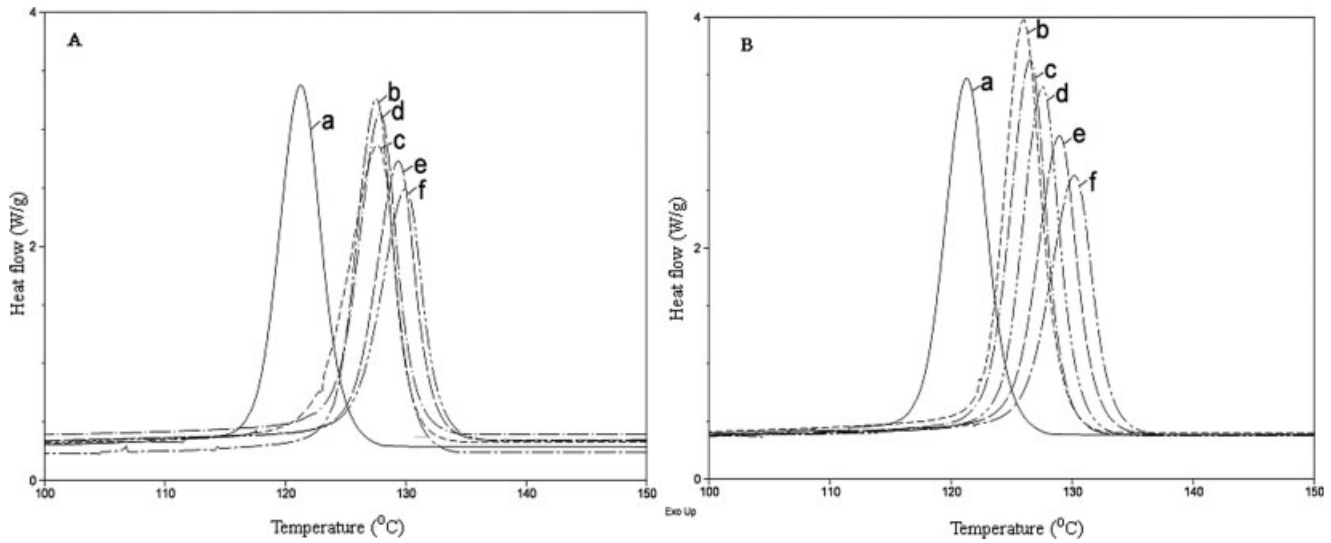

Figure 3 DSC thermograms show the crystallization of PP/*p*-talc (A) and PP/*s*-talc (B) composites during a cooling route with various talc contents: (a) 0 wt.%; (b) 9 wt %; (c) 16.7 wt %; (d) 23.1 wt %; (e) 28.6 wt %; (f) 33.3 wt %.

sion of *p*-talc in the PP matrix. This uniform dispersion and orientation is expected to enhance the mechanical properties of composites.

Crystallization analysis by DSC and MDSC

The crystallization temperature (T_c) of the pure PP was found to be 121°C. With the presence of *p*-talc, the crystallization temperatures, obtained during cooling, increased to more than 126°C, as shown in Figure 3(a). This indicates that the inorganic talc acts as a nucleating agent for PP.[10] The cooling routes of *s*-talc filled PP composites are illustrated in Figure 3(b) for comparison. It seems from the crystallization temperatures that the silane treatment does not have a significant influence on PP crystallization temperature beyond what is found for *p*-talc.

MDSC data of a PP/*p*-talc composite incorporated with 9 wt % *p*-talc are shown in Figure 4 as an illustration. The estimated values of X_c in the *p*-talc and *s*-talc filled composites are shown in Table I and Table II, respectively. The crystallinity of pure PP is 31%. The incorporation of *p*-talc—over all ranges of composition—makes the PP crystallinity in composites

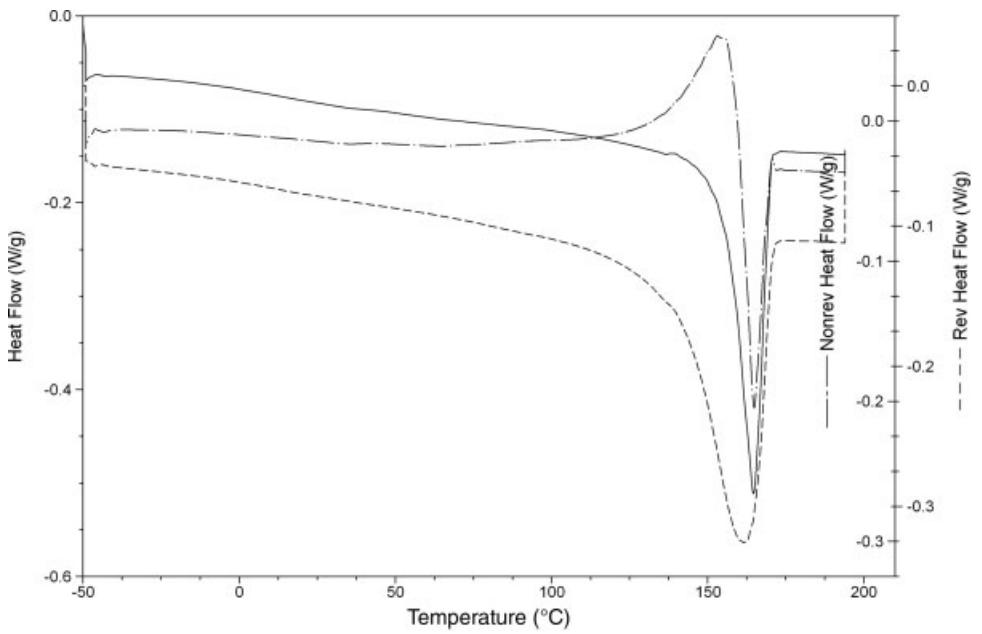

Figure 4 MDSC thermograms for PP/*p*-talc composite (9 wt % *p*-talc) illustrate reversible (short dashed line), nonreversible (long-dash/short dash line) and total heat flow (solid line).

TABLE I
Crystallization Parameters of PP/*p*-talc Composites

Parameters					
p-talc content/%	T_C/°C	ΔH_C/J/g	T_m/°C	ΔH_{diff}/J/g	X_c/%
0.0	121	84	162	65	31
9.0	127	91	165	74	35
16.7	128	109	164	91	44
23.1	128	94	164	81	39
28.6	129	88	165	78	37
33.3	129	85	164	76	36

higher than in pure PP. This result is attributed to the nucleating effect of *p*-talc.[10] Note that PP crystallinity does not always increase with increasing *p*-talc content but it is somewhat lower at higher talc contents. This result can be explained by the idea that at high *p*-talc incorporation content, the matrix phase regions are disrupted by the finely dispersed *p*-talc filler. Since crystallization is confined to smaller regions in the PP matrix, crystallinity cannot increase any more in these smaller regions even though more nucleating agent exists. Another noticeable trend in Table I and Table II is that above the maximum crystallinity, there is a more gradual decrease in the crystallinity of PP filled by *s*-talc in comparison to *p*-talc. This difference may be because at high *s*-talc content, the coupling agent compensates for the loss in polymer chain mobility resulting from the presence of *s*-talc. Greater chain mobility enables PP crystallization in composites with higher contents of *s*-talc. A similar conclusion about the effects of silane on the matrix morphology has been drawn by Li et al.[26] referring to the HDPE/talc system.

Dynamic mechanical properties

The following analysis will compare dynamic mechanical properties of PP/*p*-talc and PP/*s*-talc composites. Figure 5(a) shows the evolution of storage modulus of composites with increasing talc contents at room temperature (20°C). For either PP/*p*-talc or PP/*s*-talc composites, both moduli increase with increasing filler content, because the talc is a stiffer material compared with PP.[29] The storage moduli of either PP/*p*-talc or PP/*s*-talc are more than 100% higher when the talc concentration is around 30 wt %. There are negligible differences in the values of the dynamic moduli of PP/*p*-talc and PP/*s*-talc composites. Only at high talc content, *s*-talc filled PP composites show higher storage modulus. This might be the contribution of silane agent which helps to transfer stress at the talc-PP interface. A key result is that the two types of talc show a similar reinforcing effect.

The addition of filler sometimes results in a higher glass transition temperature, because the polymer mobility is believed to be decreased near the interface with an inorganic material.[26] Experimental results shown in Figure 5(b) illustrate, however, that PP/talc composites have a lower T_g compared to pristine PP. Considering the nucleating effect of talc determined by DSC, this unusual T_g depression can be explained. In our DSC thermograms, higher *p*-talc or *s*-talc content induced a greater T_c value, thus crystallization velocity is higher when a lower T_g value is found from DMA of the composites. The crystallization in talc filled PP when cooling from the melt starts at a temperature greater than neat PP, indicating an acceleration of the crystallization process in the presence of *p*-talc or *s*-talc. This accelerated crystallization may cause an amorphous phase when PP was short of crystallization time. This amorphous phase corresponds to a lower T_g value. A lowering of T_g was also observed by Díez-Gutiérrez et al.[29] in PP/talc composites.

Mechanical properties

Figure 6 presents the mechanical properties as a function of talc concentration measured from tensile testing. As compared with neat PP, the two types of talc composite exhibit higher tensile strengths. The maximum levels of tensile strength were obtained at 9 wt % talc for both types of talc (*p* and *s*). This maximum is followed by a decrease, yet remaining at 38 MPa at 33.3 wt % talc content, which is still higher than neat PP. With increasing talc content, the tensile modulus and strain at break show increasing and decreasing trends, respectively, as a typical effect of inorganic fillers on polymer matrix.[30]

Figure 7 illustrates three-point bending properties of various PP/talc composites. The flexural strength and flexural modulus both increase with increasing inorganic talc (*p* and *s*). Values were similar for composites prepared with both kind of talc showing that the use of *p*-talc is adequate. Figure 8 shows the variation of the impact strength as a function of talc content. For *p*-talc filled composites, a moderate increase of impact strength is seen up to 15 wt % talc content, followed by a significant increase between 15 and

TABLE II
Crystallization Parameters of PP/*s*-Talc Composites

Parameters					
s-talc content/%	T_C/°C	ΔH_C/J/g	T_m/°C	ΔH_{diff}/J/g	X_c/%
0.0	121	84	162	65	31
9.0	126	97	163	80	38
16.7	127	98	163	84	40
23.1	128	101	164	87	42
28.6	129	99	164	83	40
33.3	130	99	164	80	38

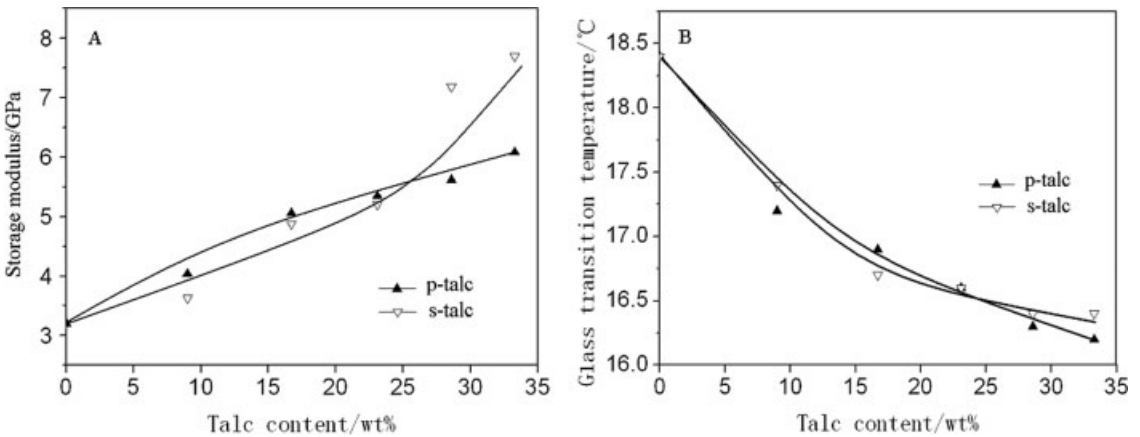

Figure 5 (A) Storage modulus of PP/*p*-talc and PP/*s*-talc composites at various talc contents at 20°C; (B) Glass transition temperature changes at various talc (*p* and *s*) contents.

23 wt %. The critical talc content leading to optimum physical properties is found to be in the region of 23 wt %. Similar behavior was observed in the case of *s*-talc composites.

In this type of composite, talc aggregation is expected at high talc concentrations. The interfacial strength between talc particles is naturally very weak compared with that of the polymer/talc interface. The decrease in impact strength that is observed here at higher talc concentrations can therefore be attributed to increased talc/talc contact in aggregates. From these results we can see that *p*-talc and *s*-talc filled PP composites show the same mechanical properties within experimental uncertainty. The silane treatment brings negligible changes. We therefore suspect that the creation of fresh surfaces of talc during the pulverization leads to the formation of a strong interface. Further evidence for this conclusion is provided by study of stress whitening.

In general, the origin of stress whitening in thermoplastic materials has been attributed to the formation of voids and microcrazing. Studies on the mechanism of crazing have suggested that the nucleation of crazes is initiated with deformation bands, and the existing voids grow into the bulk polymer by finger-like extension, linking up the stretched fibrils in their wake.[30] The increase in the fracture energy can be attributed to high energy dissipation during the crack propagation process, due to fibrillation formation between the talc and polymer ligaments.

Stress-whitened zones on the impact fracture surface of PP/*p*-talc composites are seen in the image in Figure 9. There are remnant PP fibrils, which were formed during the impact fracture, visible at the surface. The PP fibrillation in the vicinity of *p*-talc suggests effective energy transfer under stress loading, implying good interface adhesion in PP/talc composites produced by grinding process.

The pulverization process is not only a simple decrease of particle size, but also involves complicated structural and chemical changes. McCormick et al.[31] have proposed the activation of chemical reactions by milling reactants in a ball mill as a novel, low-cost method for the synthesis of a wide range of

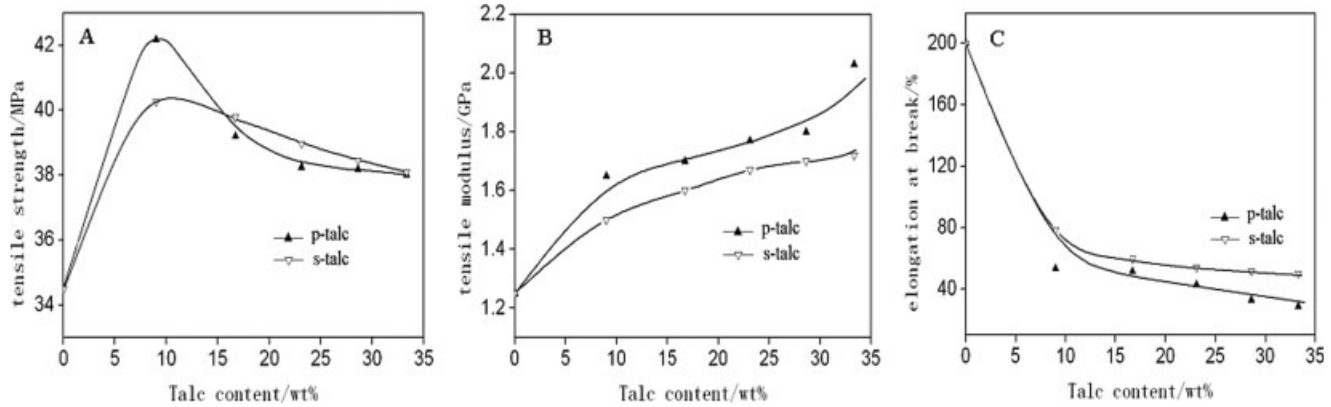

Figure 6 Tensile performance of PP/talc composite with increasing talc (*p* and *s*) content: (A) tensile strength; (B) tensile modulus; (C) elongation at break.

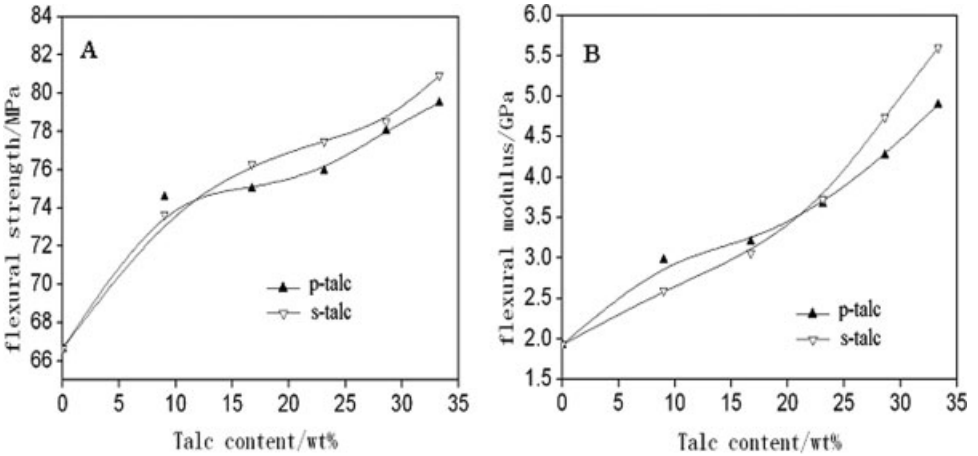

Figure 7 Flexural performance of PP/talc composites with various talc (*p* and *s*) contents: (A) flexural strength; (B) flexural modulus.

nanopowders. Frost et al.[32] modified kaolinite surfaces by mechanical and chemical treatment to produce a new surface structure of kaolinite. Yang et al.[33,34] investigated the physicochemical properties of talc powder during ultrafine grinding and found that grinding not only increases the specific area and whiteness of the talc powder, but also enhances sintering rates, allowing sintering at a lower temperature. These effects were explained by the increase of negative ζ potential, powder whiteness, wetting heat, and the decrease of the melting point.

We propose that the solid state shearing during the grinding pulverization process not only increases the surface area of talc but also facilitates physical absorption of PP chains around talc and consequently increases interfacial adhesion with the PP matrix. This novel idea of modifying inorganic fillers by grinding treatment has likewise been adopted by Xia et al.[35] to prepare polymer composites. They made a PP/carbon nanotube (CNT) composite powder by the pan milling of PP with CNTs, and speculated that the PP chain strongly bonded to CNTs, partly due to the surface modification of CNTs by the strong shearing. We cannot rule out an effect of particle size on the mechanical properties of *p*-talc/PP composites. However, regardless of the exact mechanism, the conclusion is the same. Talc modification by pulverization is simpler and faster in comparison to chemical reaction treatment, but it is just as effective.

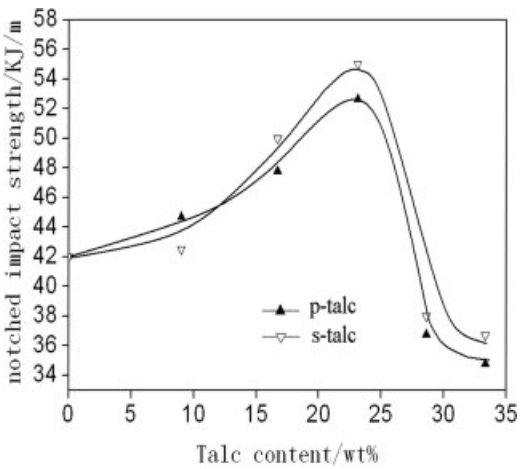

Figure 8 Notched impact strength of PP/talc composites as a function of talc (*p* and *s*) content.

CONCLUSIONS

An alternative method of modifying talc filler by grinding pulverization is applied in the fabrication of PP/talc composites. Pulverized talc particles are dis-

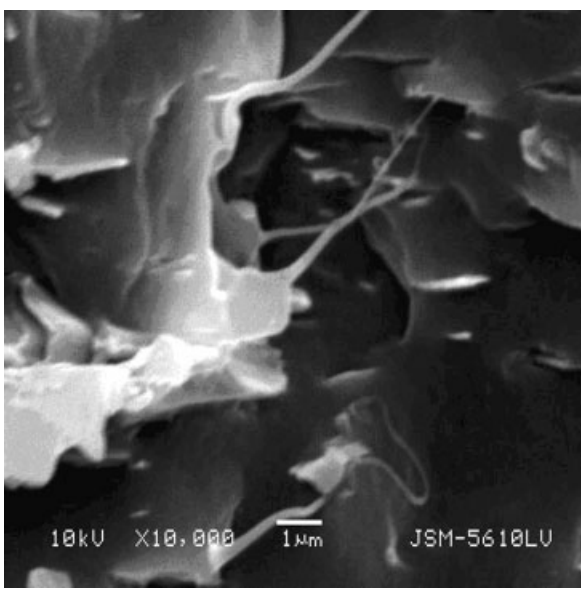

Figure 9 SEM micrograph of stress-whitened zone and fibrils in the fractured surface of PP/*p*-talc composite after impact testing at room temperature.

persed uniformly in the PP matrix with orientation from the extrusion process. The talc serves the function of nucleating PP crystallization. A reinforcing effect in the PP with *p*-talc addition is observed with dynamical mechanical analysis. The surface after impact testing indicates that PP fibrillation occurs before final fracture and hence increases energy dissipation. Various mechanical properties of composites filled by silane-treated talc are broadly the same as composites made from pulverized talc. In total, the results show that grinding pulverization is a good alternative to the chemical treatment of talc in the fabrication of PP/talc composites, because it is just as effective but simpler to use.

We acknowledge assistance from Prof Chuanxi Xiong (Wuhan University of Technology) for SEM measurement and useful discussions. We also acknowledge assistance from Prof Qing Ye (Wuhan University of Technology) for talc activation and useful discussions.

References

1. Rahma, F.; Fellahi, S. Polym Int 2000, 49, 519.
2. Ewen, J. A.; Jones, R. L.; Razavi, A.; Ferrara, J. D. J Am Chem Soc 1988, 110, 6255.
3. Setz, S.; Stricker, F.; Kressler, J.; Duschek, T.; Mulhaupt, R. J Appl Polym Sci 1996, 59, 1117.
4. Maiti, S. N.; Sharma, K. K. J Mater Sci 1992, 27, 4605.
5. Denault, J.; Vukhanh, T. Polym Compos 1992, 13, 372.
6. Roberts, D. H.; Constable, R. C.; Thiruvengada, S. Polym Eng Sci 1997, 37, 1421.
7. Stricker, F.; Bruch M.; Mulhaupt, R. Polymer 1997, 38, 5347.
8. Hadal, R. S.; Misra, R. D. K. Mater Sci Eng A 2004, 374, 374.
9. Premalal, H. G. B.; Ismail, H.; Baharin, A. Polym Test 2002, 21, 833.
10. Guerrica-Echevarria, G.; Eguiazabal, J. I.; Nazabal, J. Eur Polym J 1998, 34, 1213.
11. Denac, M.; Musil, V.; Smit, I.; Ranogajec, F. Polym Degrad Stab 2003, 82, 263.
12. Wang, W. Z.; Tang, L. X.; Qu, B. J. Eur Polym J 2003, 39, 2129.
13. Garcia-Martinez, J. M.; Laguna, O.; Areso, S.; Collar, E. P. Eur Polym J 2002, 38, 1583.
14. Albano, C.; Papa, J.; Ichazo, M.; Gonzalez, J.; Ustariz, C. Compos Struct 2003, 62, 291.
15. Rahma, F.; Fellahi, S. Polym Compos 2000, 21, 175.
16. Alonso, M.; Velasco, J. I.; deSaja, J. A. Eur Polym J 1997, 33, 255.
17. Chuah, A. W.; Leong, Y. C.; Gan, S. N. Eur Polym J 2000, 36, 789.
18. Qiu, W. L.; Mai, K. C.; Zeng, H. M. J Appl Polym Sci 2000, 13, 2974.
19. Qiu, W. L.; Luo, Y. J.; Luo, S. G.; Tan, H. M. J Beijing Institu Techn 1998, 7, 345.
20. Kunita, M. H.; Rinaldi, A. W.; Girotto, E. M.; Radovanovic, E.; Muniz, E. C.; Rubira, A. F. Eur Polym J 2005, 41, 2176.
21. Srinivasa Rao, G. S.; Choudhary, M. S.; Naqvi, M. K; Rao, K. V. Eur Polym J 1996, 32, 695.
22. Lu, D. P.; Guan, R. Polym Int 2000, 49, 1389.
23. Gaylord, N. G.; Mishra, M. K. J Polym Sci Polym Lett Ed 1983, 21, 23.
24. Velasco, J. I.; deSaja, J. A.; Martinez, A. B. J Appl Polym Sci 1996, 61, 125.
25. Alonso, M.; Gonzalez, A.; deSaja, J. A. Plast Rubber Compos Process Appl 1995, 24, 131.
26. Li, T. Q.; Liu, G. C.; Qi, K. J Appl Polym Sci 1998, 67, 1227.
27. Ivanov, I.; Muke, S.; Kao, N.; Bhattacharya, S. N. Polymer 2001, 42, 9809.
28. Choi, W. J.; Kim, S. C. Polymer 2004, 45, 2393.
29. Díez-Gutiérrez, S.; Rodríguez-Pérez, M. A.; deSaja, J. A.; Velasco, J. I. Polymer 1999, 40, 5345.
30. Hadal, R. S.; Dasari, A.; Rohrmann, J.; Misra, R. D. K. Mater Sci Eng A 2004, 372, 296.
31. McCormick, P. G.; Tsuzuki, T.; Robinson, J. S.; Ding, J. Adv Mater 2001, 13, 1008.
32. Frost, R. L.; Mako, E.; Kristof, J.; Horvath, E.; Kloprogge, J. T. Langmuir 2001, 17, 4731.
33. Yang, H. M.; Qiu, G. Z.; Wang, D. Z. J Chin Ceram Soc 2002, 30, 91 (in Chinese).
34. Yang, H. M.; Qiu, G. Z. J Chin Ceram Soc 1999, 27, 580 (in Chinese).
35. Xia, H. S.; Wang, Q.; Li, K. S.; Hu, G. H. J Appl Polym Sci 2004, 93, 378.